Geomechanics and Engineering, *Vol. 25, No. 5 (2021) 417-428*
DOI: https://doi.org/10.12989/gae.2021.25.5.417

Effect of microstructure on water retention behavior of lateritic clay over a wide suction range

Pan Jin[1], Wenzhan Zhen[2], Bo Chen[*1], De'an Sun[3], You Gao[**4] and Yonglin Xiong[4]

[1]*College of Civil Engineering and Architecture, Quzhou University,78 Jiuhua Road, Kecheng District, Quzhou, Zhejiang, 324000, P. R. China*
[2]*China Railway Eryuan Engineering Group Co. LTD, Chengdu, 610031, P. R. China*
[3]*Department of Civil Engineering, Shanghai University, 99 Shangda Road, Baoshan District, Shanghai, 200444, P. R. China*
[4]*School of Civil and Environmental Engineering, Ningbo University, Ningbo, Zhejiang, 315211, P. R. China*

(Received September 15, 2020, Revised May 31, 2021, Accepted June 3, 2021)

Abstract. To investigate the effects of soil structrue and dry density on water retention behavior of lateritic clay over a wide suction range, the axial translation technique (ATT), filter paper technique (FPT) and vapour equilibrium technique (VET) were combined to obtain soil-water retention curves (SWRCs) of specimens with different structures and dry densities. Measured SWRCs indicate that the air-entry value (AEV) and descent gradient in terms of saturation degree versus suction relationship are smallest for undisturbed specimens, and are largest for pre-consolidated specimens. The SWRCs obtained from compacted specimens with different dry densities illustrate that the AEV and descent gradient of saturation degree versus suction relationship increase with increasing the dry density. However, the effects of soil structure and dry density on the water retention behavior can be negligible at high suctions, which are verified by the curves of gravimetric water content (w) verusus suction (s) coincided after a limiting suction for specimens with different structures and dry densities. In addition, the water retention behavior can be well illustrated by pore size distributions (PSDs), obtained from mercury intrusion porosimetry (MIP). The AEVs depend on the diameters that corresponding to dramatically increase in differential intruded void ratio. And the descent gradients in the saturation degree versus suction relationship depend on their distinct PSD ranges and incremental peaks in the dominant pore sizes. Furthermore, the consistences of the AEVs and limiting suctions, deduced from the PSDs and SWRCs, demonstrate that the water retention behavior is highly dependent on the PSDs, and the SWRC features can be captured well by the PSDs.

Keywords: lateritic clay; soil water retention curve; soil structure; dry density; pore size distribution

1. Introduction

The soil water retention curve (SWRC) is an important hydraulic property to reflect the soil's capacity to store and release water in unsaturated state, and it is usually presented by the suction (matric or total suction) versus gravimetric or volumetric water content, or degree of saturation (Fredlund and Rahardjo 1993). The SWRC is very important in understanding and predicting mechanical behavior of unsaturated soils, such as, compressibility, strength and permeability (Alonso *et al*. 2013, Aqtash and Bandini 2015, Rahimi *et al*. 2015, Jeong and Kim 2017, Zhang *et al.* 2018b, Gao *et al*. 2021). For this reason, the SWRCs had been attracted great attentions from the scholars over past years. Moreover, the factors affecting the SWRCs had also been extensively investigated, including soil structure (Sun *et al*. 2016), dry density (Dieudonne *et al.* 2017), aggregate size (Lipiec *et al*. 2007), drying-wetting cycles (Azizi *et al*. 2017), etc. Besides, the microstructure effect had been intensively studied, and that pore size distributions (PSDs) had been employed to illustrate the features of SWRC in recent years (Sun *et al*. 2016, Hou *et al*. 2020, Niu *et al*. 2020, Zhou *et al.* 2021).

Many beneficial conclusions on the SWRCs had been obtained from previous studies, while the measured SWRCs of lateritic clays are relatively few (Kew and Gilkes 2006, Otálvaro *et al*. 2015, Sun *et al*. 2016, Chen *et al*. 2019). Indeed, the lateritic clay, as a problematic clay for obvious fissures and significant shrinkage (Gidigaso 1972), had caused many geology hazards by the rainfall infiltration in its distribution regions (Li and Cameron 2002, Meshida 2006, Chen *et al*. 2019, Rasool and Kuwano 2020). Besides, the lateritic clay is mainly distributed in tropical or subtropical regions, and it sometimes has high suctions (low water content) in ground surface, owing to the arid climates (Miguel and Bonder 2012). Nevertheless, the investigations on the SWRCs of lateritic clay at high suctions (s>50 MPa) in existing results is fewer (Sun *et al*. 2016). Therefore, it is necessary to study the water retention behavior of lateritic clay over a wide suction range.

It is well known that the water retention behavior of soils is highly dependent on the soil microstructure, and the SWRC features can be captured well by the PSDs (Sun *et al*. 2016, Ng *et al*. 2016, Niu *et al*. 2020). Nevertheless, the bimodal and unimodal PSDs of natural lateritic clays from different countries, were reported by Miguel and Bonder

∗Corresponding author, Professor
E-mail: chen.bo@qzc.edu.cn
∗∗Corresponding author, Associate Professor
E-mail: gaoyou@nbu.edu.cn

ISSN: 2005-307X (Print), 2092-6219 (Online)

(2012) and Sun *et al*. (2016). Moreover, the SWRCs and PSDs of the lateritic clay are different for samples obtained from different regions (Miguel and Bonder 2012, Otálvaro *et al*. 2015, Sun *et al*. 2016). In addition, the variations of PSDs with soil structure and dry density for lateritic clay, and the mechanism how the PSD affects the SWRCs, are needed to be further investigated (Otálvaro *et al*. 2015, Sun *et al*. 2016). Thus, it is necessary to carry out the water retention tests and MIP tests on lateritic clay, with different soil structures and dry densities, to reveal the mechanism that how soil structure and dry density affect the SWRCs can be represented by the PSDs.

This paper presents the SWRCs of specimens with different soil structures and dry densities over a wide suction range, obtained by combining the axial translation technique (ATT), filter paper technique (FPT) and vapour equilibrium technique (VET). The effects of structure and dry density on the SWRCs of lateritic clay are illustrated by comparing the SWRCs of different specimens. Meanwhile, the variations of PSDs, obtained from the MIP tests on the specimens of lateritic clay, with different structures and dry densities, are intensively studied to investigate how the PSD affects the SWRC. Based on a close relationship between the SWRCs and PSDs, it can be concluded that the SWRC is highly dependent on its PSD, and the main features (e.g., AEV and descent gradient) of the SWRCs can be well captured by the PSDs of lateritic clay.

2. Testing material and specimen preparation

2.1 Testing material

Undisturbed cubic samples (20 × 20 × 20 cm) of tested lateritic clay were trimmed from 1.5 m below the ground surface by the block sampling method, with the objective to reduce the effect of disturbance on soil structure. The detailed sampling site is located in Quzhou city, which is about 200 km northwest from Hangzhou, the capital of Zhejiang province in China. The detailed sampling site is shown in Fig.1. Moreover, the obtained intact natural soil samples are representative lateritic clay in Jinhua-Quzhou basin, and its basic physical properties are shown in Table 1. Besides, the X-ray diffraction (XRD) demonstrates that the main mineral composition of tested lateritic clay contains montmorillonite, illite and kaolinite. Also, the hematite and gibbsitethe are detected in the tested lateritic clay. The X-ray fluorescence (XRF) illustrates that the predominant chemical oxides are silicon oxide (SiO_2) and aluminum oxide (Al_2O_3), as well as a small quantity of iron II oxide (Fe_2O_3) is detected in tested clay (Wang 2020).

2.2 Specimens preparation

Undisturbed specimens for the tests were trimmed by cutting ring (d=61.8mm, h=20.0 mm), and specimens were saturated by the vacuum saturation technique before drying tests with suction-controlled methods. The aim of saturating specimens is to reduce the difference in initial states (e.g., water content, saturation degree) of undisturbed specimens used in the ATT, FPT and VET. Indeed, the SWRCs will be

Table 1 Physical properties of tested lateritic clay

Physical property	Value	Grain size distribution	
Specific gravity	2.73	Sand (%)	15.7
Liquid limit (%)	41.1	Silty (%)	39.4
Plastic limit (%)	18.5	Clay (%)	44.9
Natural water content (%)	18.2-22.7	Swelling and shrinkage	
Maximum dry density (Mg/m^3)	1.68	Free swelling ratio (%)	28
Optimum water content (%)	17.9	Volumetric shrinkage (%)	10

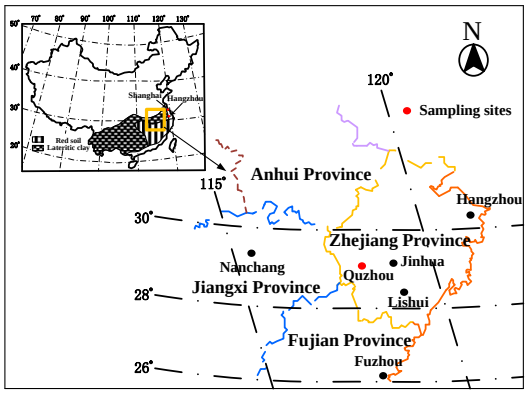

Fig. 1 Detailed sampling site of tested lateritic clay

obviously different for specimens with different initial states, caused by the difference in the PSDs (Burton *et al.* 2014, Otálvaro *et al*. 2015, Zhang *et al*. 2018a). Moreover, the SWRCs of natural lateritic clays obtained from different regions were reported to be unimodal or bimodal, due to their different PSDs (Miguel and Bonder 2012; Sun *et al*. 2016). Thus, to reduce the difference in the PSDs of natural lateritic specimens used in different techniques (ATT, FPT and VET), which may be caused by their different initial states (e.g., water content, void ratio, etc.), the undisturbed specimens are all saturated before the drying tests.

The pre-consolidated sample was prepared as a method suggested by Burland (1990), i.e., the lateritic clay slurry with gravimetric water content of 2.0 w_L (w_L is liquid limit), was poured into a stainless-steel cylinder with the diameter of 15.0 cm and height of 16.0 cm. Then, the consolidation pressure was applied to 70 kPa (close to the dry density of 1.50Mg/m^3) by multi-stage loading. The sample was pushed out from cylinder after the completion of consolidation, and the pre-consolidated specimens were trimmed from the sample by cutting ring (d=61.8 mm, h=20.0 mm). Obtained pre-consolidated specimens were saturated at initial state, thus, the specimens can directly be used in the drying tests over a wide suction range.

Compacted specimens were prepared as follows: de-aerated water was sprayed on dried powders of lateritic clay until water content reached 12%, which is smaller than the optimum water content (w_{opt}=17.9%). The reason to select 12% as initial water content is that the water contents corresponding to initial dry density of compacted specimen at 1.65 Mg/m^3 are 12% and 21%. The large soil aggregates will be formed when the powders are mixed with high water content (21%). And it is impossible to break down large soil

aggregates when specimens were compacted at a dry density of 1.35 Mg/m^3. Besides, the effect of initial water content on the SWRCs can be eliminated after compacted specimens were saturated. The thoroughly mixed powder was sealed in plastic bags for 24 hours, to ensure added de-aerated water distribute uniformly in the clay. Then, the prepared clay was placed in a molder with inner diameter of 61.8 mm and height of 20.0 mm, and it was compacted to specimens with dry densities of 1.35, 1.50 and 1.65 Mg/m^3, respectively. Because specimens compacted at the dry side of optimum water content exhibit bimodal PSDs (Delage *et al*. 1996), the SWRCs for soils with two pore populations are distinct (Zhang *et al*. 2018a). For this reason, compacted specimens in tests were all saturated by vacuum saturation technique before the drying tests, to ensure compacted specimens used in different techniques (e.g., ATT, FPT, VET) have the same initial states.

3. Testing methods and procedure

In order to obtain the SWRCs over a wide suction range, the ATT and VET were combined to control the suctions. Meanwhile, the FPT was employed to measure the suctions of specimens with different gravimetric water contents. The detailed procedures of above-mentioned techniques are as follows.

Fig. 2 Pressure plate apparatus used in tests

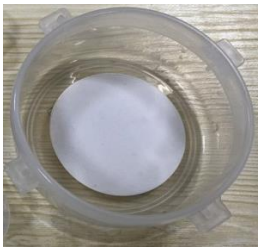

(a) Contact filter papers placed

(b) Tested specimen placed

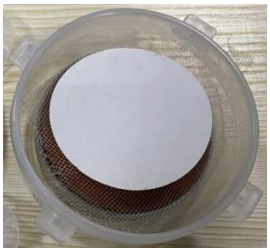

(c) Isolate filter paper placed

(d) Tested specimen sealed

Fig. 3 Filter paper techniques

Fig. 4 Vapor equilibrium technique used in tests

Axial Translation Technique (ATT)

The ATT is based on the principle that the matric suction can be controlled by the air pressure if the pore water pressure in the specimen is maintained to atmospheric pressures (Hoyos *et al*. 2008). Therefore, the desired suction can be applied by controlling the air pressure in the pressure plate apparatus (Fig. 2). The ATT can only control the suctions from 0 to 1.5 MPa, for the highest AEV of ceramic disk in the pressure plate apparatus is 15 bars (1.5 MPa). During the drying tests, saturated specimen with cutting ring was put on saturated ceramic disk, and air pressures were applied by step and step. When the equilibriums of water and deformation were reached, the weight and volume of specimens were measured to determine the gravimetric water content and dry density (void ratio) at each stage.

Filter Paper Technique (FPT)

The FPT, as an effective way to determine matric and total suctions simultaneously, can measure the suctions from 0.1 to 100 MPa (Leong *et al*. 2002, Bonder and Miguel 2012, Sun *et al*. 2016). The detailed procedures in the tests were shown in Fig. 3, i.e., specimens were air-dried to desired gravimetric water contents, and a single Whatman No.42 filter paper was inserted between two filter papers with larger diameters to protect the paper from contamination. The sandwiched filter papers were placed on the bottom of specimens, keeping the sandwiched filter papers in intimate contact with the soil specimens in a sealed box (see Fig. 3). At the same time, another filter paper was put on clean plastic strainer to measure the total suction. The objective of putting the plastic strainer on the specimen was to isolate the filter paper and specimen. The specimen was then sealed in lock-lock box to reach water and vapor equilibriums in 2 weeks at temperature of 22 ºC (ASTM 2007). The gravimetric water contents of the filter papers, water contents and volumes of soil specimens were measured after the suction equilibrium. According to the calibration curves of the gravimetric water content versus suction for the filter paper by Leong *et al*. (2002), the matric and total suctions of soil specimens can be calculated by Eqs. (1)-(3) and Eqs. (4) and (5), respectively.

$$\lg\psi = 2.909 - 0.0229 w_f \qquad (w_f \geq 47) \tag{1}$$

$$\lg\psi = 4.945 - 0.0673 w_f \qquad (26 \leq w_f \leq 47) \tag{2}$$

Table 2 Saturated salt solution and corresponding suction

Saturated salt solution	*RH*(%)	Total suction(MPa)
LiBr	6.6	367.54
LiCl·H2O	12.0	286.70
CH_3COOK	23.1	198.14
$MgCl_2·6H2O$	33.1	149.51
K_2CO_3	43.2	113.50
NaBr	59.1	71.12
KI	69.9	48.42
NaCl	75.5	38.00
KCL	85.1	21.82
$Na_2SO_3·7H_2O$	90.8	13.10
K_2SO4	97.6	3.29

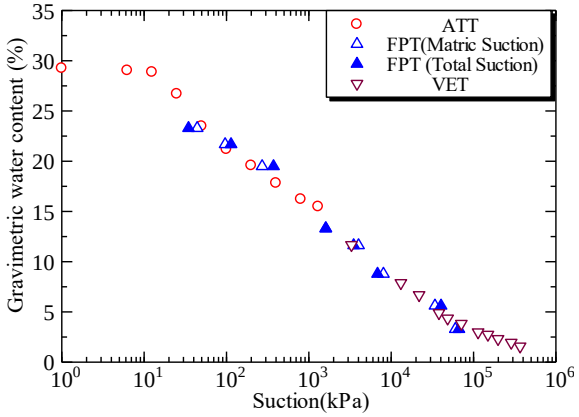

(a) *w*-*s* curve

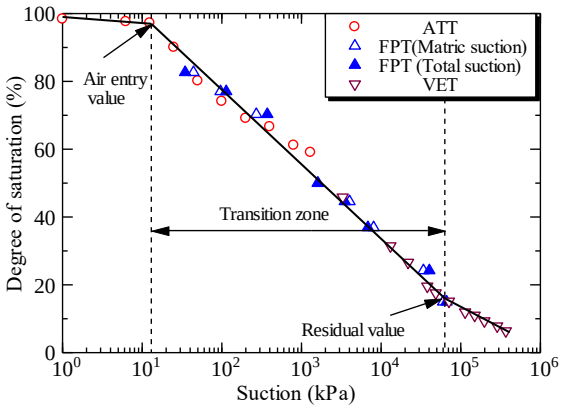

(b) S_r-*s* curve

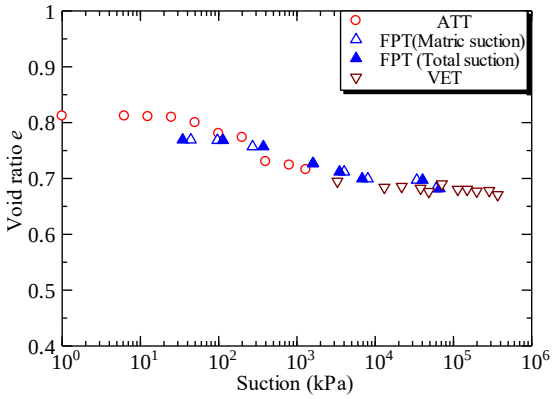

(c) *e*-*s* curve

Fig. 5 Water retention behavior of natural lateritic clay over a wide suction range technique

$$\lg\psi = 5.310 - 0.0879w_f \qquad (w_f < 26) \qquad (3)$$

$$\lg\psi = 8.778 - 0.2220w_f \qquad (w_f \geq 26) \qquad (4)$$

$$\lg\psi = 5.310 - 0.0879w_f \qquad (w_f < 26) \qquad (5)$$

where w_f is the gravimetric water content of the filter paper, and ψ is matric or total suction.

Vapor Equilibrium Technique (VET)

The VET can well control the high suctions (3.29~367 MPa) by sealing specimens in the desiccators with different saturated salt solutions (Fig. 4). The suctions applied to the specimens is thorough the equilibrium of vapor potential between specimen and saturated salt solution in enclosed space (Blatz *et al*. 2008). The detailed relative humidity of saturated salt solution and corresponding suctions at 20°C are listed in Table 2 (Greenspan 1977).

With the objective to decrease the suction equilibrium time by the VET in the drying tests, saturated specimens (*d*=61.8 mm, *h*=20mm) used in the VET were cut to eight pieces, and each two pieces were sealed in one desiccator.

Table 3 Comparing the calculated and measured suctions for specimens with different structures and dry densities

Specimen	Dry density (Mg/m^3)	e	e_{mf}	d_a (μm)	s_{ae} (kPa)	s_{ad} (kPa)	d_c (μm)	s_{ce} (kPa)	s_{cd} (kPa)	d_r (μm)	s_{re} (MPa)	s_{rd} (MPa)
U	1.51	0.812	0.708	19.8	14.5	13.2	0.25	1152	1120	0.01	28.8	55.1
C	1.50	0.822	0.685	6.9	41.7	40.6	0.25	1152	1120	0.01	28.8	42.3
P	1.51	0.808	0.660	4.4	65.4	68.5	0.25	1152	1120	0.01	28.8	25.4
C1	1.35	1.022	0.764	10.9	26.4	21.8	0.32	900	800	0.01	28.8	38.1
C	1.50	0.822	0.685	6.4	45.0	40.6	0.32	900	800	0.01	28.8	42.3
C2	1.65	0.654	0.600	4.3	66.9	76.8	0.32	900	800	0.01	28.8	45.7

Note: e is the void ratio measured physically from specimens; e_{mf} is the intruded void ratio by MIP; d_a, d_r are diameters corresponding to AEV and residual suction value; d_c is the limiting diameter corresponding to the limiting suction; s_{ae}, s_{ce}, s_{re} are the suctions calculated from Eq. (6); s_{ad}, s_{cd}, s_{rd} are the suctions deduced from the SWRCs

One piece was used to determine gravimetric water content, and the other piece was used to measure the volume of irregular lateritic clay. After the equilibrium of water and vapor was reached, the volumes of small pieces with different suctions were measured by the liquid displacement, suggested by Péron *et al*. (2007) and Sun *et al*. (2016). Then, the variations of gravimetric water content and void ratio with suction were obtained.

Mercury Intrusion Porosimetry (MIP)

The PSDs of specimens with different soil structures and dry densities were obtained by the MIP tests, and the procedures are as follows. (1) The representative portions of specimens with different soil structures and dry densities, were cut into small cubes with about $1cm^3$ in volume; (2) The small cubes were hydrated by the freeze-drying method, suggested by Griffiths and Joshi (1989) and Delage *et al*. (1996), to reduce negative influence on the microstructure during the specimen preparation. (3) The hydrated cubes were intruded by mercury from low to high pressures step by step, and the cumulative curves of intruded void ratio versus entrance pore sizes (0.005~350 μm) can be obtained from the MIP tests.

4. Results of SWRCs over a wide suction range

4.1 SWRCs obtianed by combined techniques

Fig. 5 shows the SWRCs of undisturbed lateritic clay specimens in the drying tests, obtained by using different testing techniques (ATT, FPT, VET), and the information of tested undisturbed specimens (dry density, void ratio) is shown in Table 3. The letters U, C and P in Table 3 represent undisturbed, compacted and pre-consolidated specimens, respectively, and the meaning of symbols shown in the following figures are the same. The variations of gravimetric water content (w), degree of saturation (S_r) and void ratio (e) with the suction are shown in Figs. 5(a)-5(c), respectively. The coincidences of water retention (w-s; S_r-s) and deformation (e-s) in the overlapped suction ranges with different techniques, mean that the combined techniques are effective to measure the SWRCs over a wide suction range. Besides, the coincidence of matric and total suctions at the same gravimetric water content or saturation degree, simultaneously measured by FPT, indicates that there is no osmotic suction (salinity) existing in tested lateritic clay.

Fig. 5 shows that the SWRCs of undisturbed specimen are typical curves with conventional ‘‘S” shape. The AEV and residual value deduced from the S_r-s curve in Fig. 5(b) are 13.2 kPa and 55.1 MPa, respectively. It is worth noting that the AEV and residual value were determined from the SWRCs by a graphical method, i.e., the reflection points of two tangent lines in boundary effect zone and transition zone, transition zone and residual zone (Sun *et al.* 2016). The gravimetric water content and saturation degree decrease to 1.54% and 7.91% when the suction reaches 367 MPa. The results are close to the conclusion that the gravimetric water content and saturation degree of clays will be zero at the suction of 1000 MPa (Vanapalli *et al*. 2000). Besides, Fig. 5(c) shows that void ratio decreases with increasing suction, and it is more obvious at low to medium suctions (s<1.2 MPa). The variation of void ratio with suction is similar with results reported by Ng *et al*. (2016) and Sun *et al*. (2016). It had been reported that two AEVs were observed in transition zone of the SWRCs from lateritic clays, which is caused by the bimodal PSDs of clay (Miguel and Bonder 2012), as well as the cracks generated by the shrinkage of lateritic clay specimens (Sun *et al*. 2016). Indeed, if there is no fissure existing in soils, only one AEV can be observed for unimodal PSDs, and two AEVs can be observed in soils with two population of pores (Sun *et al*. 2016; Zhang *et al*. 2018a). For the reason that undisturbed specimens used in the tests are saturated and intact without cracks, and the saturated specimen often exhibits unimodal PSDs (Burton *et al.* 2014; Otálvaro *et al*. 2015), the SWRCs of tested undisturbed lateritic clay are typical curve with one AEV.

4.2 SWRCs for specimens with different structures

Fig. 6 shows the SWRCs of specimens with different soil structures, which is caused by the different specimen preparation methods, at the same initial dry density of 1.50 Mg/m^3. Figs. 6(a) and 6(b) show that the SWRCs of different specimens are typical curves with conventional ‘S’ shape. Nonetheless, the AEVs and residual values are different for specimens with different soil structures. It can be deduced from Fig. 6(b) that the AEVs for undisturbed, compacted and pre-consolidated specimens are 13.2, 40.6 and 65.4 kPa, respectively. The difference in the AEV

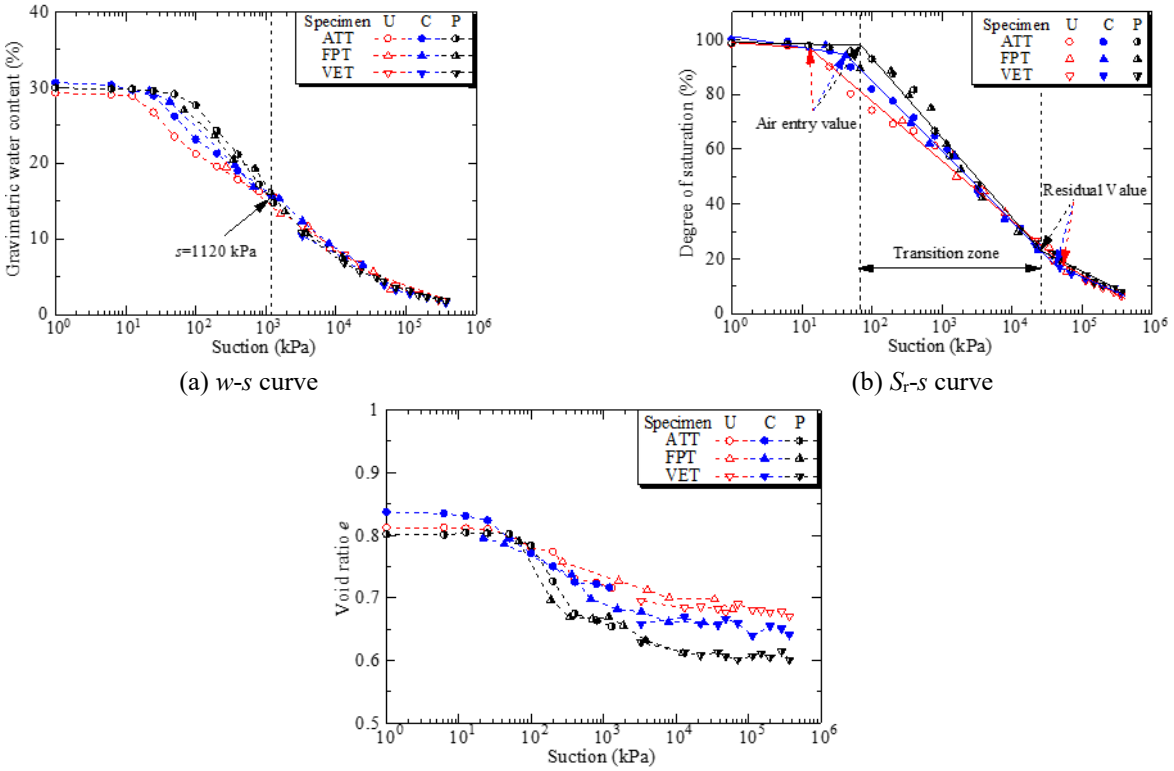

(a) *w*-*s* curve (b) S_r-*s* curve

(c) *e*-*s* curve

Fig. 6 Water retention behavior of specimens with different structures over a wide suction range

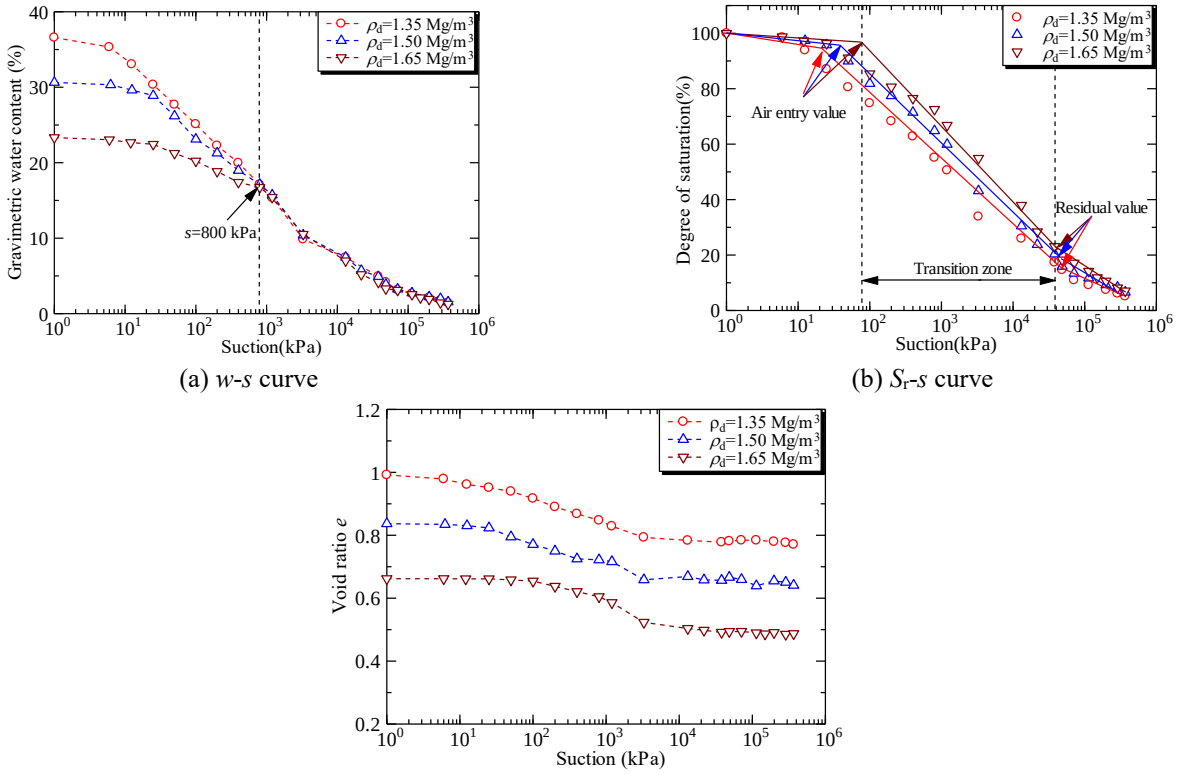

(a) *w*-*s* curve (b) S_r-*s* curve

(c) *e*-*s* curve

Fig.7 Water retention curves of specimens with different dry densities over a wide suction range

among different specimens can be attributed to the difference in the PSDs of specimens, and the PSDs in compacted or pre-consolidated specimen is more uniform than undisturbed specimen. It is because the extra-large pores in the compacted or pre-consolidated specimen will be eliminated by the specimen reconstruction (Burton

et al. 2014, Ng *et al*. 2016).

It is worth noting that the AEV of pre-consolidated specimen is almost the same as its consolidation pressure. It is because the PSDs will be greatly affected by the applied loading in the early, while the AEV is highly dependent on the PSDs. The residual values deduced from the S_r-s curves in Fig. 6(b) are 55.1, 42.3 and 25.4 MPa for undisturbed, compacted and pre-consolidated specimens, respectively. The distinct difference in residual value can be attributed to the different loss of saturation degree with increasing the suction. Meanwhile, it can be seen from Fig. 6(b) that the descent gradient of the saturation degree versus suction relationship is smallest for undisturbed specimen, while it is largest for pre-consolidated specimen.

It needs to note that the gravimetric water content versus suction relationships for different specimens are almost the same after the limiting suction (the suction that *w*-*s* curves from different specimens begin to coincide) of 1120 kPa, as shown in Fig. 6(a). Moreover, the difference in the saturation degree versus suction relationships for different specimens tends to be slight in the very high suction ranges (Fig. 6b).

Ng *et al*. (2016) and Sun *et al*. (2016) had also reported that the variation of gravimetric water content or saturation degree with suction is the same for the undisturbed and compacted specimens in high suction ranges, due to the same distribution of micro-pores in tested clay. Besides, the coincidences of gravimetric water content and saturation degree versus suction in different specimens mean that the influence of soil structure on water retention behavior can be negligible at very high suctions, despite the effect of soil structure on residual value of the SWRCs cannot be neglected.

Fig. 6(c) shows that the variations of void ratio with suction are distinct for undisturbed and pre-consolidated specimens. And the void ratios are largest and smallest for the undisturbed and pre-consolidated specimens at the same suction, because the minimum and maximum shrinkage occurred in undisturbed and pre-consolidated specimens. However, the variations of void ratio with suction are almost the same for the compacted and pre-consolidated specimens, and the difference in void ratio at the same suction is mainly caused by their different initial void ratio. In addition, it is worth noting that the reduction of void ratio is obvious at low suction ranges, while reduction is slight at high suctions in the drying tests. The result is consistent with the reduction of void ratio with suction in other clays (Otálvaro *et al.* 2015, Ng *et al*. 2016, Sun *et al*. 2016, Niu *et al*. 2020). Furthermore, the suctions corresponding to the change of variation tendency in void ratio is about 0.4 MPa, and that it is the same for specimens with different soil structures.

4.3 SWRCs for specimens with different dry densities

Fig. 7 shows the SWRCs of specimens with different dry densities, and gravimetric water content (w), degree of saturation (S_r) and void ratio (e) versus suction are shown in Figs.7(a)-7(c), respectively. It needs to be illustrated that only two suction-controlled techniques (e.g., ATT and VET) were used in the tests. It is because the SWRCs over a wide suction range can be obtained by interpolating the curves between suctions of 1.5 and 3.29 MPa. Fig.7(a) shows that although the initial gravimetric water content is highest for specimen with dry density of 1.35 Mg/m^3, the *w*-*s* curves of specimens with different dry densities are coincident when the suction exceeds the limiting suction (s= 800 kPa). It means that the dry density has negligible effect on the gravimetric water content if suction is larger than limiting suction. Romemo *et al*. (1999) and Dieudonne *et al.* (2017) had also reported similar test results, obtained from the compacted Boom clay and bentonite clay.

Fig. 7(b) indicates that the AEV is higher for larger dry density. It shows that the AEV increases from 21.8 to 76.8 kPa gradually when the dry density varies from 1.35 to 1.65 Mg/m^3. Besides, the S_r-s curve of the specimen with dry density of 1.65 Mg/m^3 beyond that of specimen with lower dry density at the same suction. It means that the specimen with higher dry density will have higher saturation degree. Furthermore, the descent gradient of saturation degree is larger for specimen with higher dry density, attributed to larger loss of the gravimetric water content for specimen with higher dry density. Despite the difference in saturation degree among different specimens narrows with increasing the suction, the difference in the saturation degree cannot be eliminated at high suctions, even though the suction is high up to 367 MPa. It is because the difference in void ratio for different specimens is still obvious at high suctions. At the same time, the residual value continues to increase with increasing the dry densities, the same to the conclusions obtained by Romero *et al*. (1999). The variations of void ratio with suction for specimens with different dry densities are shown in Fig.7(c). It shows that the *e*-*s* curves are almost parallel for specimens with different dry densities, despite the difference in initial void ratio is distinct for different specimens. It is mainly because the dry density has no effect on the shrinkage of lateritic clay, reported by Tan *et al*. (2015) and Wang (2020). In addition, the reduction of void ratio is significant at low suctions, while the loss of void ratio with suction can be negligible at high suctions, which is the same to the results obtained by Ng *et al*. (2016) and Sun *et al*. (2016).

5. Results from MIP tests

5.1 PSDs of specimens with different structures

Fig. 8 shows the cumulative and differential intruded void ratio of the saturated specimens with different soil structures, and the detailed intruded void ratio (e_m) and measured void ratio (e) are listed in Table 3. It can be seen that the difference in intruded void ratio and measured void ratio is obvious, attributing to reason that the closed pores, extra-small pores (d<0.005 μm) and extra-large pores (d>350 μm) can't be detected by MIP (Delage *et al*. 1996). By reasons that the extra-large pores in compacted or pre-consolidated specimens are eliminated during specimen reconstruction, while their intruded void ratios are also about 80% of measured void ratios. Therefore, it can be

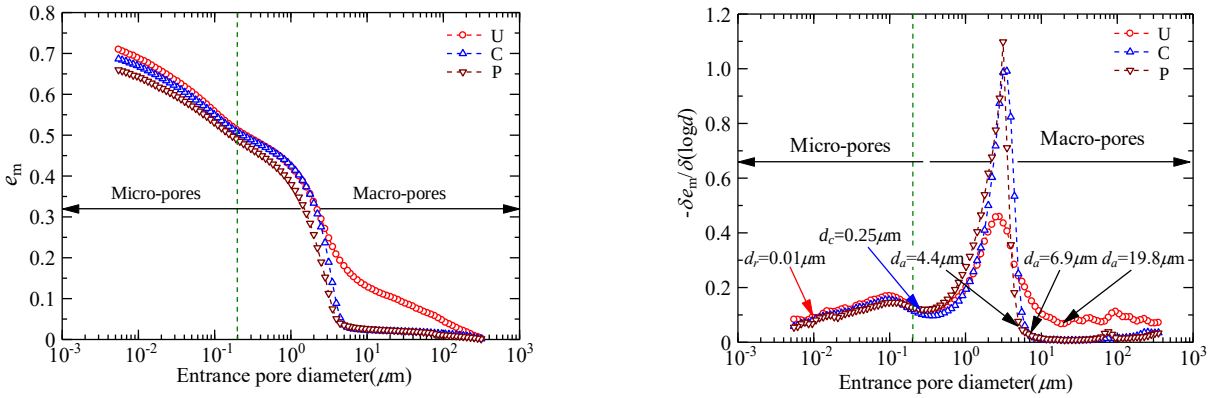

(a) Cumulative intruded void ratio (b) Differential intruded void ratio

Fig. 8 PSDs of specimens with different structures

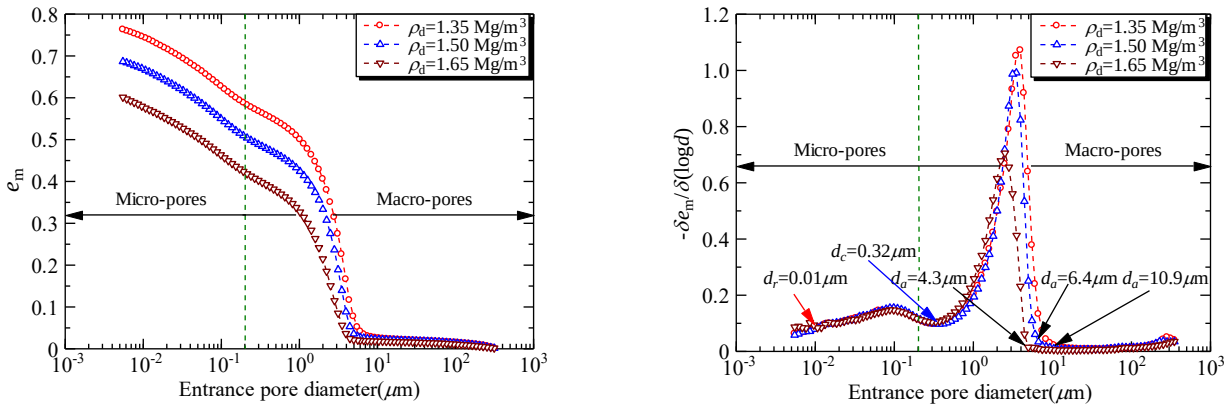

(a) Cumulative intruded void ratio (b) Differential intruded void ratio

Fig. 9 PSDs of specimens with different dry densities

concluded that the difference in measured and intruded void ratio is mainly caused by the extra-small pores, owing to the existing of montmorillonite and illite in tested lateritic clay. Lubelli *et al*. (2013) had also reported that the higher content of montmorillonite and illite, the greater difference in intruded and measured void ratios. In addition, a number of small micro-pores (d<0.01 μm) existing in tested lateritic clay can be verified from the MIP test results. For instance, the cumulative intruded void ratio continues to increase with increasing pressure and it is not flattening out when the pores less than 0.01 μm.

The differential PSDs in Fig. 8(b) indicates that the PSDs of saturated specimens with different structures are all unimodal. Based on the diameter that corresponding to free or nonconstricted porosity can be selected as the delimiting diameter (Delage and Lefebvre 1984), and the determined delimiting diameter by using the above method is 0.18 μm for tested lateritic clay. In addition, the delimiting diameter for the lateritic clay from Brazil was suggested as 0.3 μm (Otálvaro *et al*. 2015). Therefore, the delimiting diameter for macro- and micro-pores is selected as 0.2 μm, Despite the unimodal PSDs exhibit in different specimens, the dominant PSDs are distinct for specimens with different structures. The distribution of dominant pore sizes for undisturbed specimen is wider than that of compacted or pre-consolidated specimen, while the incremental peak of dominant pore sizes in undisturbed specimen is obviously lower than that of compacted or pre-consolidated specimen. Meanwhile, comparing with compacted specimen, pre-consolidated specimen has narrower distribution and higher incremental peak in the dominant pore sizes.

It is worth noting that differential PSDs of undisturbed specimen is away from the coordinate axis of entrance pore diameter, which means that the pores are distributed in the full pore size range. By contrast, the differential PSDs of compacted or pre-consolidated specimens is close to the coordinate axis of entrance pore diameter at large pores (d>7 μm). The above result indicates that there are large pores existing in undisturbed specimens, and they are eliminated by the specimen reconstruction. On the contrary, the micro-pores are not affected by specimen reconstruction, which can be verified by the coincidence of micro-pores for undisturbed and remolded specimens.

5.2 PSDs of specimens with different dry densities

Fig. 9 shows the cumulative and differential intruded void ratio of the saturated specimens with different dry densities. It can be seen from Table 3 that the intruded void ratio is smaller than measured void ratio for all specimens, due to closed pores and undetectable pores by the MIP. Besides, the intruded void ratio increases with decreasing

the dry density, attributing to larger void ratio for specimen with lower dry density. In the same way, the cumulative intruded void ratio continues to increase and never flatten out at small micro-pores (d<0.01 μm), it further confirms that there are a number of undetectable pores existing in the specimens of tested lateritic clay.

The differential intruded void ratio shown in Fig. 9(b) indicates that the PSDs of specimens with different dry densities are all unimodal, due to saturation of specimens. The dominant pore sizes are mainly distributed between 0.5 and 10.9 μm, nevertheless, the diameters corresponding to dramatically increase and incremental peak in the PSDs are different. It is worth noting that there is slight difference in incremental peak for specimens with dry densities of 1.35 and 1.50 Mg/m^3. This is because many macro-pores were not detected in the specimen with dry density of 1.35Mg/m^3, which is verified by great difference in the intruded and measured void ratios (Table 3). Besides, the incremental peak of dominant pore sizes declines and shifts to left with increasing the dry density, nonetheless, the distributions of micro-pores are coincident for specimens with different dry densities. The results indicate that the dry density has only great effect on the macro-pores, which is consistent to the results obtained by Romemo *et al*. (1999) and Dieudonne *et al*. (2017). In addition, the variation of PSDs with the dry density is similar with the test results observed in other soils subjected higher vertical stress progressively (Burton *et al*. 2014). This is because the higher dry density is realized by increasing compacted force during specimen preparation, and the process is similar with applying the vertical loading on the specimens gradually. Therefore, variations of the PSDs with dry density and vertical stress are similar.

6. Discussion

The effects of soil structure and dry density on the water retention behavior have been intensively investigated, and some useful conclusions are known (Romero *et al*. 1999, Sun *et al*. 2016, Ng *et al*. 2016, Dieudonne *et al*. 2017, Hou *et al*. 2020). In fact, the effects of above factors on the SWRCs can be attributed to different microstructures in specimens, and it can be illustrated by the PSDs of soils. Furthermore, the features of SWRCs can be well presented by the PSDs of soils (Ng *et al*. 2016, Hou *et al*. 2020, Niu *et al*. 2020). Therefore, the influences of soil structure and dry density on the SWRCs can be discussed from the soil microstructure (e.g., PSD).

6.1 Effect of soil structure on SWRCs

The water in soils is expelled from macro- to micro-pores gradually, therefore, the features (e.g., AEV, descent gradient, residual value) of SWRCs can be well presented by the PSDs (Miguel and Bonder 2012, Ng *et al*. 2016, Zhang *et al*. 2018a). In addition, the AEV in SWRCs is corresponding to the diameter at which pores dramatically increase in differential PSDs (Ng *et al*. 2016, Niu *et al*. 2020). Fig. 8(b) shows that the maximum diameters (d_a) that dramatically increase in the differential intruded void ratio, which are corresponding to the AEV of undisturbed and pre-consolidated specimens, are maximum and minimum for three types of soil structure. Thus, the AEVs are lowest and highest for undisturbed and pre-consolidated specimens. Meanwhile, the descent gradient of saturation degree versus suction relationship is smallest for undisturbed specimen, owing to its lowest incremental peak of dominant pore sizes. In the same way, the largest descent gradient of pre-consolidated specimen can be owing to the highest incremental peak of differential intruded void ratio. In addition, when suction exceeds the limiting suction in Fig. 6(a), the same gravimetric water content for specimens with different structures can be attributed to the same distribution of the pores smaller than 0.25 μm in different specimens.

The mercury intrusion to porous medium, is a similar process of air injection in saturated soils in the drying tests (Sun *et al*. 2016, Niu *et al*. 2020, Hou *et al*. 2020). Thus, the suctions (AEV, residual value) can be deduced from the corresponding diameters by the Young-Laplace equation (Diamond, 1970) as

$$s = u_a - u_w = 4\sigma_w \cos\alpha / d \tag{6}$$

where s is suction; u_a is the air pressure, u_w is the water pressures; σ_w is surface tension at air-water interface, and it was treated as 0.072 N/m at 20°C (Fredlund and Rahardjo 1993); α is the contact angle between solid and water, and assumed to be 0° in the calculation; d is the pore diameter.

The detailed maximum diameters (d_a) for dramatically increase in differential PSDs are 19.8, 6.9 and 4.4 μm for the undisturbed, compacted and pre-consolidated specimens, respectively. The corresponding AEVs can be calculated by Eq. (6), and the detailed suctions are listed in Table 3. The coincidence of AEVs deduced from PSDs and SWRCs (Table 3), illustrates that the AEV of specimen can be well captured by the PSDs. At the same time, the diameter where the differential PSDs of soils begin to coincide is defined as the limiting diameter (d_c), which is corresponding to the limiting suction in this paper. The limiting diameter for the specimens with different structures is 0.25 μm, as shown in Fig. 8(b), which means that the pores smaller than 0.25 μm are the same for the specimens with different soil structures. Correspondingly, the gravimetric water content will be the same for different specimens when the suction exceeds the limiting suction. The detailed limiting suctions calculated by using Eq. (6) are shown in Table 3, and they are close to the suction deduced from the SWRCs shown in Fig. 6(a).

The residual value is corresponding to the minimum diameter (d_r) in dominant pore sizes for unimodal PSDs, as suggested by Niu *et al*. (2020). However, the suggestion is suitable for soils that the pores smaller than the minimum diameter of dominant pore sizes, can be negligible. On the contrary, numerous micro-pores existing in tested lateritic clay, which can be verified by tiny peak shown in micro-pores at 0.1 μm (Fig. 8b). Thus, selecting 0.01 μm as the diameter corresponding to residual value is more reasonable (Ng *et al*. 2016, Niu *et al*. 2020). The residual values calculated from the PSDs are listed in Table 3, and it can be

seen from Table 3 that the residual values calculated from the PSDs are not close to the residual values deduced from the SWRCs. Moreover, the calculated residual values from PSDs for different specimens are identical, different to the residual values deduced from the SWRCs. It is because the effect of different relationships of saturation degree versus suction on the determination of residual values of lateritic clay, cannot be illustrated by the PSDs.

6.2 Effect of dry density on SWRCs

The differential PSDs in the Fig. 9(b), indicates that the maximum diameter for dramatically increase in the macro-pores, corresponding to the AEV of lateritic clay, continues to decrease with increasing the dry density. Therefore, the AEV continues to increase with increasing the dry density. For the same reason, the descent gradient of saturation degree versus suction relationship continues to increase with an increase in the dry density, attributed to a narrower distribution in the dominant pore sizes. Besides, Fig. 9(b) shows that the differential PSDs of specimens with different dry densities coincide at diameter of 0.32 μm (d_c=0.32 μm), it means that pore size (d<0.32 μm) existing in compacted specimens with different dry densities are identical. Thus, the gravimetric water content for specimens with different dry densities are the same when the suctions exceed the suction calculated from the diameter of 0.32 μm, due to the same distribution of pores smaller than 0.32 μm.

As shown in Fig.9(b), the detailed maximum diameters for dramatically increase in differential intruded void ratio are 10.9, 6.4 and 4.3 μm, for the compacted specimens with dry densities of 1.35, 1.50 and 1.65 Mg/m^3, respectively. And the detailed suctions (AEVs) calculated by Eq. (6), listed in Table 3, are close to the AEVs deduced from the SWRCs in Fig.7(b). At the same time, the limiting suction calculated from the limiting diameter (d_c) are listed in Table 3. The calculated suction is also close to the suction deduced from the *w*-*s* curves in Fig. 7(a). In the same way, the diameter corresponding to the residual value is also selected as 0.01 μm. Correspondingly, the residual values calculated from the PSDs of clays, listed in Table 3, are different from residual values deduced from the SWRCs. It needs to be emphasized that the identical residual value calculated from the PSDs indicates that the PSDs can't well capture the residual value of SWRCs for the lateritic clay, owing to the existence of numerous micro-pores.

7. Conclusions

The ATT, FPT and VET were combined to investigate the SWRCs of undisturbed, compacted and pre-consolidated lateritic clay over a wide suction range, together with the PSD measurements of specimens with different structures and dry densities by the MIP. The main conclusions are as follows.

The smooth transition of the SWRCs from low to high suctions indicates that the combined techniques (ATT, FPT and VET) are effective ways to investigate the soil water retention behavior over a wide suction range. Furthermore, no difference in matric and total suctions indicates that there is no osmotic suction (salinity) in tested lateritic clay.

The difference in SWRCs for specimens with different structures indicates that soil structure has great effect on the water retention behavior at low to medium suctions. Such as, the AEV and descent gradient are smallest for undisturbed specimens, while they are largest for pre-consolidated specimens. By contrast, the influence of soil structure on the water retention behavior can be negligible at high suctions, owing to the coincidence of gravimetric water content of different specimens at the same suctions after the limiting suctions.

The SWRCs of compacted specimens with different dry densities illustrate that the AEV and descent gradient continue to increase with increasing the dry density. At the same time, the coincidence of gravimetric water content versus suction relationship after the limiting suction means that the dry density only has great influence on gravimetric water content at low suctions (s<800 kPa). In addition, the similarity in the variations of void ratio with suction for specimens with different dry densities means that the dry density has no effect on the shrinkage of lateritic clay.

The saturated specimens with different soil structures and dry densities all exhibit unimodal PSDs. However, the narrower distribution and higher incremental peak in the dominant pore size indicate that the pores in compacted or pre-consolidated specimens are more uniform. Only large pores detected in undisturbed specimens mean that large pores are eliminated by the specimen reconstruction. The incremental peak declines and shifts to left in dominant pore size of compacted specimens with increasing the dry density, which means that the dominant pore sizes become less and smaller with increasing the dry density gradually. However, the coincidence of the micro-pores for different specimens indicates that the dry density has no effect on the micro-pores of lateritic clay.

The difference in SWRCs of specimens with different structures and dry densities can be well illustrated by the PSDs. The AEVs depend on the maximum diameters where the differential intruded void ratio dramatically increases, and the descent gradients depend on the PSD ranges and incremental peaks in the dominant pore sizes. Besides, the coincidences of AEVs and the limiting suctions, deduced from the PSDs and SWRCs, demonstrate that the main features of the SWRCs can well captured by the PSDs. However, the residual suction value cannot be well captured by the PSDs of tested lateritic clay, which can be attributed to the existence of numerous micro-pores.

Acknowledgments

This study is supported financially by Public Welfare Technology Research Projects of Zhejiang Province (No. LGG19E080002), the National Natural Science Foundation of China (No. 41902279) and Natural Science Foundation of Zhejiang Province (LY19E080012).

References

Alonso, E.E., Pinyol, N.M. and Gens, A. (2013), "Compacted soil

behavior: initial state, structure and constitutive modelling". *Géotechnique*, **63**(6), 463-478. https://doi.org/10.1680/geot.11.P.134.

Aqtash, U.A. and Bandini, P. (2015), "Prediction of unsaturated shear strength of an adobe soil from the soil-water characteristic curve", *Constr. Build. Mater.*, **98**, 892-899. https://doi.org/10.1016/j.conbuildmat.2015.07.188.

ASTM Standard D 5298-03, (2007), Standard test method for measurement of soil potential (suction) using filter paper. ASTM International, West Conshohocken, Pennsylvania, U.S.A

Azizi, A., Jommi, C. and Musso, G. (2017), "A water retention model accounting for the hysteresis induced by hydraulic and mechanical wetting-drying cycles", *Comput. Geotech.*, **87**, 86-98. https://doi.org/10.1016/j.compgeo.2017.02.003.

Blatz, J.A., Cui, Y.J. and Oldecop, L. (2008), "Vapour equilibrium and osmotic technique for suction control", *Geotech. Geol. Eng.*, **26**(6), 661-673. https://doi.org/10.1007/s10706-008-9196-1.

Burland, J.B. (1990), "On the compressibility and shear strength of natural clay". *Géotechnique*, **40**(3), 329-378. https://doi.org/10.1680/geot.1990.40.3.329.

Burton, G.J., Sheng, D.C. and Campbell, C. (2014), "Bimodal pore size distribution of a high-plasticity compacted clay", *Geotech. Lett.*, **4**, 88-93. https://doi.org/10.1680/geolett.14.00003.

Chen, Y.H., Li, B.Y., Xu, Y.T., Zhao, Y.P. and Xu, J. (2019), "Field study on the soil water characteristics of shallow layers on red clay slopes and its application in stability analysis", *Arab. J. Sci. Eng.*, **44**, 5107-5116. https://doi.org/10.1007/s13369-018-03716-3.

Delage, P. and Lefebvre, G. (1984), "Study of the structure of a sensitive Champlain clay and of its evolution during consolidation", *Can. Geotech. J.*, **21**(1), 21-35. https://doi.org/10.1139/t84-003.

Delage, P., Audiguier, M., Cui, Y.J. and Howat, M.D. (1996), "Microstructure of a compacted silt", *Can. Geotech. J.*, **33**(1), 150-158. https://doi.org/10.1139/t96-030.

Dieudonne, A.C., Vecchia, G.D. and Charlier, R. (2017), "Water retention model for compacted bentonites", *Can. Geotech. J.*, **54**(7), 915-925. https://doi.org/10.1139/cgj-2016-0297.

Diamond, S. (1970), "Pore size distribution in clays", *Clay Clay Miner.*, **18**(1), 7-23. https://doi.org /10.1346/CCMN.1970.0180103.

Fredlund, D.G. and Rahardjo, H. (1993), *Soil Mechanics for Unsaturated Soils*, John Wiley and Sons Inc., New York, U.S.A.

Gao, Y., Li, Z., Sun, D.A. and Yu, H.H. (2021), "A simple method for predicting the hydraulic properties of unsaturated soils with different void ratios", *Soil Till. Res.*, **209**, 104913. https://doi.org/10.1016/j.still.2020.104913.

Gidigaso, M.D. (1972), "Mode of formation and geotechnical characteristics of laterite materials of Ghanan in relation to soil forming factors", *Eng. Geol.*, **6**(2), 79-150. https://doi.org/10.1016/0013-7952(72)90034-8.

Griffiths, F.J. and Joshi, R.C. (1989), "Change in pore size distribution due to consolidation of clays", *Géotechnique*, **39**(1), 159-167. https://doi.org/10.1680/geot.1989.39.1.159.

Greespan, L. (1977), "Humidity fixed points of binary saturated aqueous solutions", *J. Res. National Bureau Standards*, **81**(1), 89-96. https://doi.org/10.6028/jres.081A.011.

Hou, X.K., Qi, S.W., Li, T.L., Guo, S.F., Wang, Y., Li, Y. and Zhang, L.X. (2020), "Microstructure and soil-water retention behavior of compacted and intact silt loess", *Eng. Geol.*, **277**, 105814. https://doi.org/10.1016/j.enggeo.2020.105814.

Hoyos, L.R., Laloui, L. and Vassalo, R. (2008), "Mechanical testing in unsaturated soils", *Geotech. Geol. Eng.*, **26**, 675-689. https://doi.org/10.1007/s10706-008-9200-9.

Jeong, S.S. and Kim, Y.M. (2017), "Modeling of shallow landslides in an unsaturated soil slope using a coupled model", *Geomech. Eng.*, **13**(2), 353-370. http://doi.org/10.12989/gae.2017.13.2.353.

Kew, G. and Gilkes, R. (2006), "Classification, strength and water retention characteristics of lateritic regolith", *Geoderma*, **136**, 184-198. https://doi.org/10.1016/j.geoderma.2006.03.025.

Leong, E.C., He, L. and Rahardjo, H. (2002), "Factors affecting the filter paper method for total and matric suction measurements", *Geotech. Test. J.*, **25**(3), 1-12. https://doi.org/10.1520/GTJ11094J.

Li, J. and Cameron, D.A. (2002), "A case study of a courtyard house damaged by expansive soils", *J. Perform. Constr. Fac.*, **16**(4), 169-175. https://doi.org/10.1061/(ASCE)0887-3828(2002)16:4(169).

Lipiec, J., Walczak, R., Witkowska-Walczak, B., Nosalewicz, A., Słowińska-Jurkiewicz, A. and Sławiński, C. (2007), "The effect of aggregate size on water retention and pore structure of two silt loam soils of different genesis", *Soil Till Res.*, **97**(2), 239-246. https://doi.org/10.1016/j.still.2007.10.001.

Lubelli, B., Winter, D.A.M., Post, J.A., Van-Hees, R.P.J. and Drury, M.R. (2013), "Cryo-FIB-SEM and MIP study of porosity and pore size distribution of bentonite and kaolin at different moisture contents", *Appl. Clay Sci.*, **80-81**, 358-365. https://doi.org/10.1016/j.clay.2013.06.032.

Meshida, E.A. (2006), "Highway failure over talc-tremolite schist terrain: A case study of the Ife to Ilesha highway, South Western Nigeria", *B. Eng. Geol. Environ.*, **65**(4), 457-461. https://doi.org/10.1007/s10064-005-0037-7.

Miguel, M.G. and Bonder, B.H. (2012), "Soil-water characteristic curves obtained for a colluvial and lateritic soil profile considering the macro and micro porosity", *Geotech. Geol. Eng.*, **30**, 1045-1420. https://doi.org/10.1007/s10706-012-9545-y.

Niu, G., Shao, L.T., Sun, D.A. and Guo, X.X. (2020), "A simplified directly determination of soil-water retention curve from pore size distribution", *Geomech. Eng.*, **20**(5), 411-420. https://doi.org/10.12989/gae.2020.20.5.411

Ng, C.W.W., Sadeghi, H., Hossen, B., Chiu, C.F., Alonso, E.E. and Baghbanrezvan, S. (2016), "Water retention and volumetric characteristics of intact and re-compacted loess", *Can. Geotech. J.*, 53(8), 1258-1269. https://doi.org/10.1139/cgj-2015-0364.

Otálvaro, I.F., Neto, M.P.C. and Caicedo, B. (2015), "Compressibility and micro- structure of compacted laterites". *Transp. Geotech.*, 5:20-34. http://doi.org/10.1016/j.trgeo.2015.09.005

Péron, H., Hueckel, T. and Laloui, L. (2007), "An improved volume measurement for determining soil water retention curves", *Geotech. Test J.*, **30**(1), 1-8. https://doi.org/10.1520/GTJ100167.

Rahimi, A., Rahardjo, H. and Leong, E.C. (2015), "Effects of soil water characteristic curve and relative permeability equations on estimation of unsaturated permeability function", *Soils Found.*, **55**(6), 1400-1411. https://doi.org/10.1016/j.sandf.2015.10.006.

Rasool, A.M. and Kuwano, J. (2020), "Effect of constant loading on unsaturated soil under water infiltration conditions", *Geomech. Eng.*, **20**(3), 221-232. https://doi.org/ 10.12989/gae.2020.20.3.221.

Romero, E., Gens, A. and Lloret, A. (1999), "Water permeability, water retention and microstructure of unsaturated compacted Boom clay", *Eng. Geol.*, **54**(1-2), 117-127. https://doi.org/10.1016/S0013-7952(99)00067-8.

Sun, D.A., Gao, Y., Zhou, A.N. and Sheng, D.C. (2016), "Soil-water retention curves and microstructures of undisturbed and compacted Guilin lateritic clay", *B. Eng. Geol. Environ.*, **75**(2), 781-791. https://doi.org/ 10.1007/s10064-015-0765-2.

Tan, Y.Z., Yu, B., Liu, X.L., Wan, Z. and Wang, H.X. (2015), "Pore size evolution of compacted laterite under desiccation

shrinkage process effects", *Rock Soil Mech*., **36**(2), 369-375 (in Chinese). https://doi.org/10.16285/j.rsm.2015.02.010.

Vanapalli, S.K., Wright, A. and Fredlund, D.G. (2000), "Shear strength behavior of a silty soil over the suction range from 0 to 1,000,000 kPa", *Proceedings of the 53rd Canadian Geotechnical Conference*, Montreal, Canada, October.

Wang, J. (2020), "Study on the hydro-mechanical behaviors and microstructure of lateritic clay over a wide suction range", M. Sc. Thesis, Shanghai University, Shanghai, China.

Zhang, F., Cui Y.J. and Ye, W.M. (2018a), "Distinguishing macro- and micro-pores for materials with different pore populations", *Geotech*. *Lett*., **8**, 1-9. https://doi.org/10.1680/jgele.17.00144.

Zhang, F., Cui Y.J., Zeng, L.L., Robinet, J.C., Conil, J. and Talandier J. (2018b), "Effect of degree of saturation on the unconfined compressive strength of natural stiff clays with consideration of air entry value", *Eng*. *Geol*., **237**, 140-148. https://doi.org/10.1016/j.enggeo.2018.02.013.

Zhou, X.Y., Sun, D.A. and Xu, Y.F. (2021), "A new thermal analysis model with three heat conduction layers in the nuclear waste repository", *Nucl*. *Eng*. *Des*., **317**, 110929. https://doi.org/10.1016/j.nucengdes.2020.110929.

IC